JOURNAL OF SPACECRAFT AND ROCKETS
Vol. 41, No. 4, July–August 2004

Shape Correction of Inflatable Membranes by Rigidization and Actuation

Arup Maji*
U.S. Air Force Research Laboratory, Kirtland Air Force Base, New Mexico 87117-5776
Patrick Montemerlo†
University of New Mexico, Albuquerque, New Mexico 87131-1351
and
Tang-tat Ng‡
U.S. Air Force Research Laboratory, Kirtland Air Force Base, New Mexico 87117-5776

The desire to see farther into space with increased accuracy is driving the development of large diameter (10–100 m in diameter) inflatable telescope reflectors that can be launched in a compact form and inflated in space. The surface shape of these membrane reflectors must be precise down to the micrometer level. However, it is unlikely that a membrane reflector could reach this ideal shape without the assistance of active and passive shape correction. Two methods of shape correction considered in this study were 1) passive actuation through epoxy-coating shrinkage strains during rigidization and 2) active actuation through a polyvinylidene fluoride (PVDF) piezoelectric film. Laser interferometry shearography and shadow moiré interferometry techniques were used to observe how cure stress and PVDF actuation affect the surface shape of sample membranes. The effect of in-plane strains on the reflector shape was analyzed using a finite element model. Results show that a limited amount of shape correction is possible with both techniques. However, the magnitude of shape correction diminishes dramatically with inflation pressure and is not sufficient to overcome the surface errors caused by geometric nonlinearities at high inflation pressures.

Nomenclature

E = elastic modulus for polyvinylidene fluoride (PVDF), 2.0×10^9 Pa
$E_e(t)$ = elastic modulus of the epoxy at time t, Pa
E_m = elastic modulus of the membrane, Pa
H = thickness of the membrane, m
h = thickness of the PVDF film, cm
h_e = thickness of the epoxy, cm
h_m = thickness of the membrane, cm
p = applied pressure difference, Pa
R = membrane radius, m
r_1 = radius of curvature of the membrane, cm
r_2 = normal distance to the axis of revolution, cm
s = distance from the camera to the object, cm
V = voltage applied to PVDF film, V
v = in-plane displacement, cm
w = out-of-plane displacement, cm
x = shearing direction
α = shearing angle of the birefringent crystal, deg
$\delta\varepsilon(t)$ = shrinkage strain of the epoxy at time interval δt, cm/cm
δ_{13} = piezostrain constant for PVDF film, 25×10^{-12} m/V
ε = strain in PVDF film, cm/cm
ε_{eff} = shrinkage strain on the membrane due to the curing of an epoxy on one side of it, cm/cm
ε_θ = circumferential strain in membrane, cm/cm
ε_ϕ = meridian strain in membrane, cm/cm
ζ = observation angle, deg
θ = illumination angle, deg
λ = wavelength of the laser, cm
ϕ = angle between the local normal and the axis of revolution of the membrane, deg

Received 20 October 2002; revision received 20 January 2004; accepted for publication 29 January 2004.

*Senior Research Scientist, VSSV; arup.maji@Kirtland.af.mil. Member AIAA.
†Research Assistant, Department of Civil Engineering.
‡Associate Professor, Department of Civil Engineering.

Introduction

CURRENTLY, the diameter of space telescopes is limited by the diameter of the space vehicle, commonly the space shuttle, used to launch the telescope. To meet the desire to see farther into space with increased resolution, it is required that the diameter of telescope reflectors be increased dramatically. One option would be to create a large inflatable reflector that could be brought into space, inflated, and rigidized for use.[1] Large inflatable reflectors from 10 to 100 m in diameter are of interest to the U.S. Air Force for future space-based radar, imaging optics, solar concentrators, etc. (Fig. 1). Such a new class of structures could offer vastly improved resolution and lower cost to orbit. Similarly, there is a need for radio frequency antennas for communication and space-based radar that are larger than 50 m in diameter while possessing 1–2-mm rms surface accuracy over the aperture.[2] However, it is well known that the deviation in shape of an inflated membrane compared to an ideal parabolic surface, referred to as the W error,[3] is caused by geometric nonlinearities associated with large deformations during inflation. Therefore, practical inflatable rf and optical reflectors must incorporate some means of compensating for such errors in surface shape.

Furthermore, requirements of the defense community make it necessary for large imaging apertures to have adequate stiffness to mitigate excessive vibration in the vacuum environment of space. Indeed, stiffness is a major criterion for the joint NASA/Department of Defense Advanced Mirror System Demonstrator program that is developing mirrors for deployable telescopes.[4] Thus, large inflatable reflector structures must be rigidized in space to provide structural stiffness and stability. The typical approach to rigidization involves inflation of a partially cured composite membrane and subsequent on-orbit curing of the membrane material. As such, meeting the necessary surface accuracy through inflation and rigidization requires a better understanding of the mechanics of membrane structures and the interaction between cure shrinkage and surface deformations.

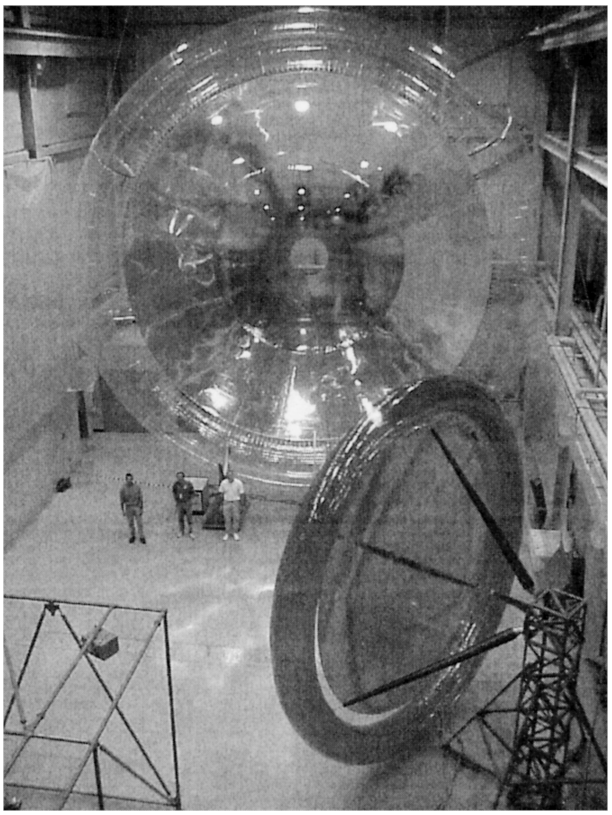

Fig. 1 Large (9-m) inflatable reflectors at the U.S. Air Force Research Laboratory (SRS Corp.).

Significant advances have been made on the development of inflatable rigidizable structures.[5] A number of possible rigidization methods such as the sub-Tg (glass-transition temperature) method and ultraviolet-cure method have been identified. Although studies have been conducted to explain how epoxy behaves as it cures and how it acts on a single fiber as it cures, no research has been done on the question of how shrinkage strains and other characteristics of epoxy curing affect the shape of an inflated composite structure. It is believed that the differential shrinkage during rigidization can be coupled with variations in membrane thickness to reduce the W error, but achieving positive results requires that the process is accurately understood and experimentally quantified.

The idea of using polyvinylidene fluoride (PVDF) for actuating membrane surfaces to reduce shape errors has matured in recent years.[6] By applying opposing voltages on either side of a free-standing two-layer (BiMorph) system, one can induce significant curvature in the system. Maji and Starnes used PVDF in an attempt to actuate and correct the shape of a 51-cm (20-in.) inflated membrane.[7] It was proven that, whereas shape actuation of a few micrometers is possible, the low actuation force of PVDF makes it unsuitable for correcting the millimeter level surface inaccuracies that result from the W error. Therefore the basic premise of the present research is that the membrane has to be fabricated to near net-shape before any residual corrections can be made through PVDF actuation or rigidization.

There are two primary questions addressed in the research reported here:

1) How much shape correction is possible through cure shrinkage at rigidization?

2) How much shape correction is possible through PVDF actuation of a membrane that is prefabricated to near net shape and, hence, needs very little inflation pressure?

Experimental Setup

Figure 2 shows the test setup for the present study. A stainless steel vacuum chamber 31.8 cm (12.5 in.) long and 14.9-cm (5.875-in.) inside diameter was fabricated and assembled on the optics table to inflate the membrane. The membrane test specimen was stretched over one end of the vacuum chamber and forced into a reflector shape by vacuum pressure. The flanges at the two ends of the chamber were 20.3 cm (8 in.) in diameter. The flange at the rear end had a blank steel plate with a valve connected to a mechanical pump. This flange was connected by a series of bolts and sealed with a copper O-ring. It was connected to a pressure gauge by means of a rubber hose connected to a threaded fitting on the side of the flange. The range of this absolute pressure gauge was 0–0.16 MPa (0–23 psi) with a resolution of 0.7 Pa (±0.0001 psi). Both ends of the rubber hose were wrapped with vacuum bag tape to prevent leakage.

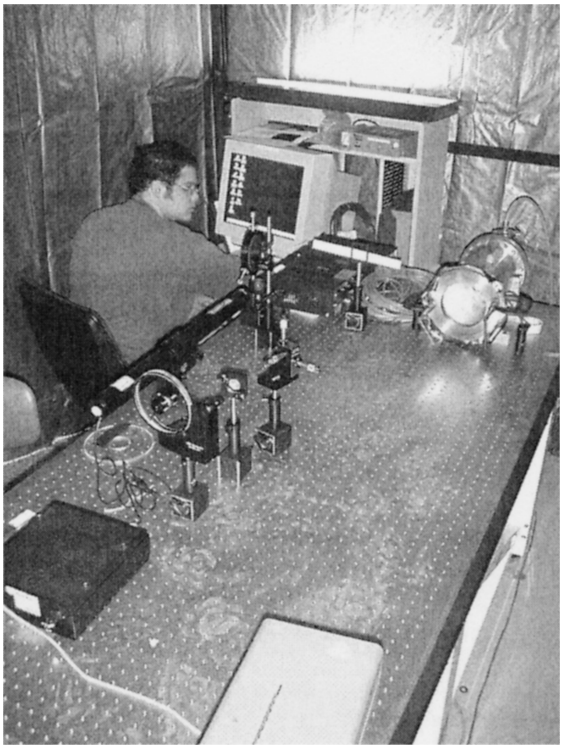

Fig. 2 Membrane inflation and interferometry test setup.

A rubber O-ring treated with vacuum grease was placed in the groove of the flange in the front of the chamber. After the membrane was installed over the rubber O-ring, a cardboard gasket was set on the outside edge of the flange and a 20.3-cm (8-in.)-diam steel ring was placed in front of it. This ring was then clamped to the flange using eight C-clamps. Clamps were used instead of bolts to provide uniform stresses on the edge of the membrane and to eliminate the need for putting holes in the membranes around the edges. The flange sat on two stainless-steel saddles that are 23.2 cm (9 1/8 in.) wide, 12.7 cm (5 in.) tall, and 2.5 cm (1 in.) thick. The saddles were attached to the optics table.

Displacement of the membrane surface was measured using interferometry, shearography, and shadow moiré techniques. The interferometry technique applied is very generic and could be changed depending on the required directional sensitivity and resolution. In this system, a charged coupled device camera was focused on the surface of the membrane, which was illuminated by a 10-mW helium–neon laser. The camera was connected to a personal computer workstation equipped with a image acquisition board. For shearography, the camera was equipped with a birefringent crystal to shear the image.[8] Image acquisition and processing was accomplished using commercially available software packages.

Shearography is an interferometric technique that is used to measure the change of shape of the surface at all points across the surface. The surface shape is related to fringes that appear in the shearographic image through

$$\frac{\partial w}{\partial x} = \frac{\lambda/(s \cdot \tan\alpha)}{\cos\theta + \cos\zeta} \tag{1}$$

The software implementation of image subtraction for shearography has been discussed elsewhere.[9]

In addition to shearography, which was used to monitor the changes in shape, the shadow moiré method (see Ref. 10) was also used to monitor the actual deformed shape of the membrane. A 10.2-cm (4-in.)-square grating plate with a grating pitch of 0.1 mm was used for this effort. Based on the illumination and observation angles, the sensitivity of the system was 0.28 mm (black fringe to black fringe).

Shape Control Through Cure Shrinkage

The use of a layer of curable epoxy to rigidize a thin inflatable PVDF membrane was studied. The objective of the experiment was to determine whether shrinkage strains caused by the curing epoxy have a significant effect on the surface shape of the inflated membrane. Two measurement techniques with significantly different resolutions (laser shearography and shadow moiré) were applied. Limitations of the experiment were quantified, and results were compared with finite element and classical analyses.

Membrane Specimen

A 28-μm-thick PVDF membrane was first cut to the appropriate size, that is, approximately 20.3 cm (8 in.) in diameter, and one side was sprayed with clear matte spray paint so that the surface was non-reflective (to facilitate shearography). For the rigidization experiments, a 7.6-cm-diam (3-in.-diam) region of the center of the membrane was coated with a 75-μm-thick layer of commercially available two-part epoxy (Epoxy Laminating Systems EZ-10). The epoxy was applied using a 15.2×15.2 cm (6×6 in.) metal stencil with a 7.6-cm (3-in.)-diam hole punched in the center. There were 100 parts of epoxy resin, that is part A, mixed with 44 parts hardener, that is, part B, by weight. The resin and hardener were stirred slowly for several minutes until fully mixed and with caution to prevent the entrapment of air bubbles in the epoxy mixture.

Experimental Limitation: Pressure Loss from Diffusion Through PVDF Membrane

Shearoraphy tests on the 28-μm-thick PVDF membranes showed consistent movement of the membrane due to loss of vacuum in the chamber at a rate of 1.3 μm/min ($\approx 2\lambda$) (Fig. 3). The pressure differentials across the membrane at the start and end of this 1-min time interval were 7302.02 Pa (1.0598 psi) and 7299.27 Pa (1.0594 psi), respectively. When Hencky's[11] approximate equation [Eq. (2)] was used the peak deflections w of the membrane were calculated to be 1.04635 and 1.04622 cm, respectively. Here R is radius, E is elastic modulus (2.0 GPa for the PVDF) and h is thickness of the membrane (28 μm). Therefore a 1.3-μm difference in displacement is expected corresponding to the 2.754 Pa (0.0004 psi) loss of vacuum over the 1-min interval:

$$w = \sqrt[3]{pR^4/3.53Eh} \tag{2}$$

It was suspected that this loss of vacuum was due to diffusion of air through the thin PVDF film (rather than leakage in the vacuum system), and the following calculation supports this hypothesis. The vacuum chamber has an internal volume of 0.0222 m^3 (1355.4 $in.^3$). A 2.754 Pa (0.0004 psi) increase in internal pressure would require the diffusion of 0.0002 g of air through the PVDF membrane. (Density of air at sea level at 0°C is 1.275 kg/m^3.) Unfortunately, no data were found on the permeability of air through PVDF. Thus, an estimate was made using permeability values for other polymeric materials.

Koerner found permeability values for water vapor diffusion through high-density polyethylene, chlorosulfonated polyethylene, and polyvinyl chloride to be 0.00013, 0.0084, and 0.013 perm · cm, respectively.[12] Because these measured permeabilities vary by two orders of magnitude, and the permeability of air is likely to be somewhat different from that of water vapor, it is impossible to use these data to estimate accurately the permeability of PVDF.

When an intermediate value of 0.0013 is assumed for the air permeability of PVDF, the permeance of a 28-μm-thick membrane would be 0.46 perm. Similarly, the mass of air that would diffuse through the membrane under the pressure differential of 7.3 kPa (1.06 psi) in 1 min is 0.0003 g. This is comparable to the measured 0.0002 g of air diffusion already discussed. Hence, the amount of vacuum loss observed through diffusion (0.0002 g/min) is quite typical of polymeric membranes.

These results indicate that it is not possible to hold a membrane stable with the vacuum chamber setup described earlier to study rigidization-induced deformation at micrometer level of sensitivity because the test would have to be stable over long periods of time for displacements induced by shrinkage to be evident. One alternative is to use a vacuum chamber of significantly greater volume so that the diffusion has a smaller impact on the internal pressure.

Shadow Moiré Measurement of Cure-Shrinkage Deformation

Because the shearography system is too sensitive, the geometric shadow moiré method (see Ref. 11) was used to monitor membrane movement in long-time-duration rigidization experiments. Figure 4 shows a moiré fringe pattern for the deformed membrane. Each moiré fringe represents 0.28 mm of out-of-plane motion of the membrane. Counting these fringes determines the deformation shape of the membrane, which can be compared with the predicted deformation from Eq. (2). This comparison gives an independent measurement of the in-plane elastic stiffness of the PVDF membrane material (2.0 GPa).

During the 4-h period while the epoxy cured on the membrane the fringe pattern did not show any significant change. (Only a fraction of a fringe movement was observed, attributable to the loss of vacuum.) Because the sensitivity of this method is considered to be one-half of a fringe, that is, 0.14 mm, it was concluded that the rigidization-induced shape change of this membrane is less 0.14 mm.

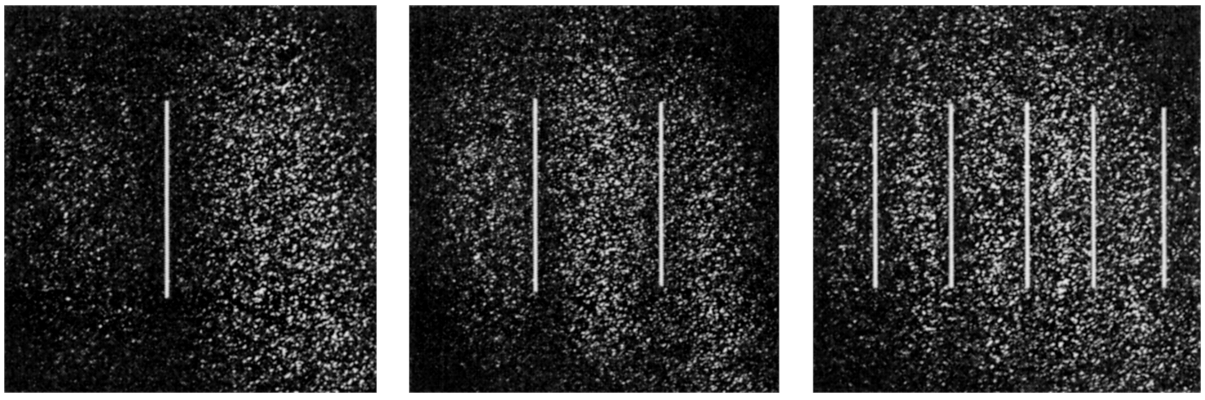

Fig. 3 Shearography fringe pattern due to loss of vacuum.

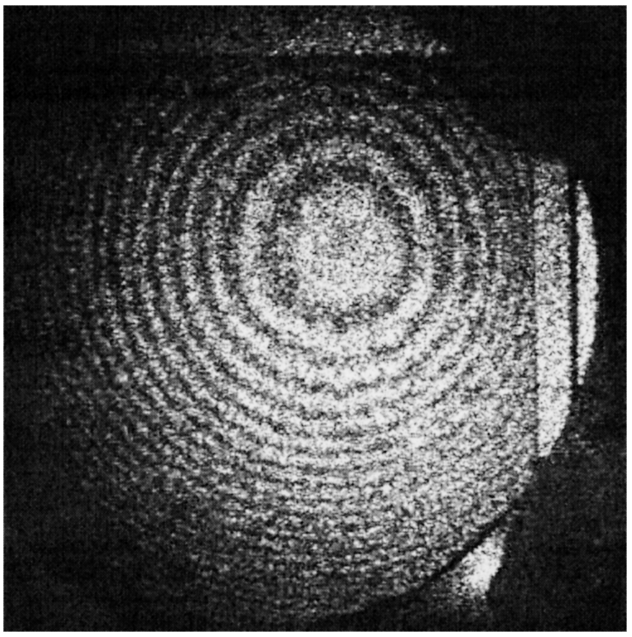

Fig. 4 Moiré fringe pattern.

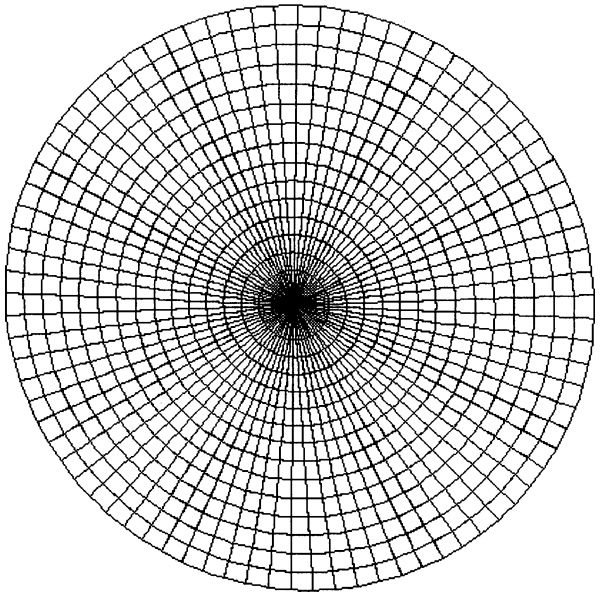

Fig. 5 Finite element mesh.

Table 1 Deformation caused by shrinkage strain

Shrinkage strain, %	Central deflection, mm
0	6.7820
0.01	6.7618
0.1	6.5819
0.25	6.2920
0.5	5.8362
0.75	5.4137
1.0	5.0292

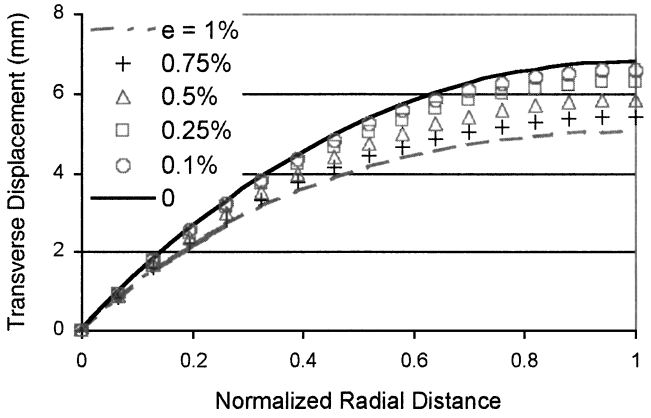

Fig. 6 Deformation of membrane.

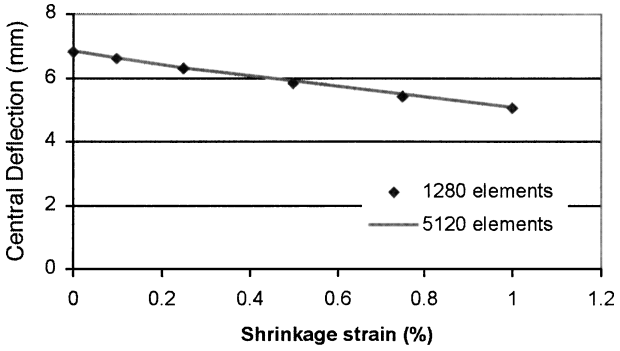

Fig. 7 Convergence study of membrane inflation.

Finite Element Analysis of Cure-Shrinkage Deformation

A finite element method (FEM) analysis was conducted to further explore the deformations due to shrinkage of the epoxy layer. The analysis was conducted using the ABAQUS finite element program that allows large deformations and that makes it possible to capture the initial inflation of a membrane surface. A 0.038-mm (0.0015-in.)-thick plane circular membrane of diameter 158.75 mm (6.25 in.) was modeled with 1536 second-order membrane elements (Fig. 5). The material properties used were $E = 2$ GPa (290 ksi) and $\nu = 0.3$, corresponding to the PVDF.

After the inflation, isotropic strains are applied to a central circular segment [76.2-mm (3-in.) diam] of the membrane representing the region where the epoxy layer was applied in the experiments. Figure 6 shows the deformation under an applied pressure differential of 2103 Pa (0.305 psi). When the central 76.2-mm circle is subject to a shrinkage strain, the deformation changes as shown in Fig. 6 and Table 1. Thus, a 0.1% strain will change the deformation by only 0.2 mm, which is less than one fringe in the shadow moiré system (0.28 mm).

A convergence study with progressive mesh refinement was done to verify the accuracy of the FEM analyses. Deformation prediction with 1280 vs 5120 elements was shown to be identical (Fig. 7). The analytical prediction of initial deflection [Eq. (2)] was 6.78 mm, the same as the FEM prediction.

Interpretation of Cure-Shrinkage-Induced Strain Data

Whereas curing of an epoxy causes shrinkage strains, such strains can change the shape of the inflated membrane only if the epoxy also has significant stiffness. Most of the cure shrinkage of epoxies occurs before they solidify and gain stiffness.[13] For example, Geuss et al. presented data documenting both the shrinkage strain and the modulus of an SL5170 epoxy as it cures.[14] Figure 8 shows that almost all of the 1.4% shrinkage of the epoxy occurs in the first 60 s, and Fig. 9 shows that the elastic modulus during that period is very small compared to the eventual elastic modulus of that epoxy. These trends are typical of most epoxy resin systems and are consistent with the result presented here, which indicate that cure shrinkage causes little change in shape of an inflated membrane.

When one of the layers in an uninflated two-layer material shrinks, it causes curvature due to the combined effect of shrinkage and stiffness. On the other hand, an inflated membrane under pressure does not sustain moment and reacts only to the resulting strain. The effective total shrinkage strain on the membrane, ε_{eff}, due to the

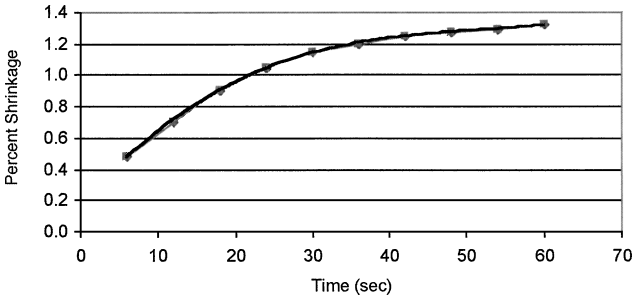

Fig. 8 Shrinkage strain vs time (Geuss et al.[14]).

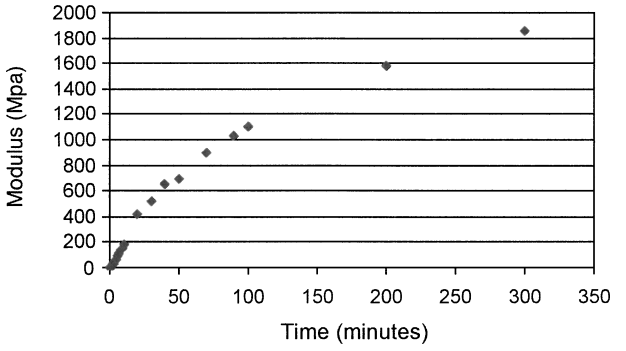

Fig. 9 Modulus vs time (Geuss et al.[14]).

curing of an epoxy on one side of it can be obtained from

$$\varepsilon_{\text{eff}} = \int_0^{\infty} \frac{E_e(t) h_e \delta\varepsilon(t)}{E_m h_m + E_e(t) h_e} \tag{3}$$

The thickness of the two materials, membrane and epoxy are h_m and h_e, respectively.

Implications for the Development of Inflatable Membrane Mirrors

Based on Eq. (3) and the data shown in Figs. 8 and 9, the effective total shrinkage strain is less than 0.1%. This is why no change in the moiré fringe pattern could be observed during the curing of the epoxy on the inflated membrane. By contrast, shrinkage due to coating stresses during rigidization could easily cause significant curvature changes in an uninflated membrane. This is because curvature is equal to strain/thickness, and the small thickness of membranes lead to large curvatures. However, the same shrinkage is unable to significantly alter the curvature of an inflated membrane.

The use of cure shrinkage for altering the inflated shape of a rigidizable membrane should be limited to reflector systems with very low inflation pressures. For such cases, it is possible to do material property tests that determine the shrinkage vs modulus data, similar to those data presented in Figs. 8 and 9, for the candidate rigidizable material. Through the use of Eq. (3), it is then possible to determine the effective shrinkage strain ε_{eff} that would cause changes to the surface profile.

Shape Control Using PVDF

The second method of shape correction investigated involved the use of a PVDF film inflated under minimal 689 Pa (0.1 psi) pressure. The actuation of BiMorph PVDF by itself, in an unrestrained experiment, can be significant.[6] The actuation of the PVDF film alone was done to demonstrate an upper bound to the amount of actuation possible, because attaching it to a second membrane material will only reduce the actuation ability, depending on their relative stiffnesses. The goal of this investigation was to investigate its ability to correct the shape of a membrane while it is inflated with minimal pressure, once again, to determine the upper bound.

The induced strain ε in a PVDF film is given by

$$\varepsilon = \delta_{31}(V/h) \tag{4}$$

where V, h, and δ_{13} ($=25 \times 10^{-12}$ m/V) are the applied voltage, thickness, and the piezostrain constant. Hence, an applied voltage of 40 V, across a 28-μm-thick PVDF membrane will induce a strain of $\approx 36\,\mu\varepsilon$. If two such PVDF layers are attached to each other to create a BiMorph, this strain would induce a curvature of $\varepsilon/h = 1.28$/m. Such curvatures are clearly visible to the naked eye, and hence, it is possible to demonstrate the actuation ability of a BiMorph PVDF without special equipment. However, because in inflated membrane is under tension and could not sustain bending, the influence of a PVDF film on the overall inflated shape is far less significant. The following test was designed to see how much out-of-plane motion could be obtained from the actuation of a single layer of PVDF to an inflated membrane with near zero in-plane tension forces.

Membrane Specimen

The shape and dimensions of the PVDF membrane were first marked out on the film and cut out with a pair of scissors. Because the scissors tend to push the metallic coatings of the PVDF together, which shorts the two sides, it is necessary to check the resistance of the PVDF across the two sides. If there is a short circuit, approximately 3 mm (1/8 in.) of the metallic coating must be removed from the circumference of the PVDF by using a chemical solvent such as acetone. The leads used to apply voltage to the PVDF were made from surgical stainless-steel sucher. The insulation was removed from either end of the wire and one side of the wire was attached to the center of the PVDF circle using conductive copper tape. The other end was left for later attachment to the voltage source. The resistance should also be checked between the end of the sucher and the metallic surface it is attached to. This ensures that there is a good connection across the one side. The membrane is then placed in the vacuum chamber, and the test was run.

The initial radius of curvature of the membrane was determined using the shadow moiré method (fringe pattern similar to Fig. 4) to be 0.45 m. The subsequent actuation of the PVDF with 40 V caused the membrane to expand, moving the center point 12 μm inward. Subsequent increase in the applied voltage to 50 V moved it by a total of 15 μm.

Influence of PVDF on Membrane Shape

Actuation of PVDF results in an in-plane strain in the membrane as per Eq. (4), which assumes that the PVDF is isotropic and the meridian and circumferential strains ε_ϕ and ε_θ are equal. For a membrane that is relatively stress free (minimal inflation pressure), the resulting displacements in the meridian (tangential) direction and the normal (out-of-plane) directions v and w are given by[15]

$$\frac{\delta v}{\delta \phi} - v \cot\phi = r_1 \varepsilon_\phi - r_2 \varepsilon_\theta, \qquad w = v \cot\phi - r_2 \varepsilon_\theta \tag{5}$$

where the variable ϕ along the membrane surface is defined as the angle between the normal to the point and the axis of revolution of the shell.

These equations demonstrate that the influence function corresponding to PVDF actuation involves a coupling between the in-plane and normal displacements v and w. The deflection of the center can be obtained from the second equation as $w = r_2\varepsilon_\theta$ because $v = 0$ at the center of the membrane, from symmetry. Therefore, the maximum shape correction (normal deflection) that can be obtained is approximately (noting that curvature varies slightly along the paraboloid) equal to the radius of curvature of the inflated membrane times the PVDF induced strain ε_θ. For the radius of curvature of 0.45 m and actuation strain of 36 $\mu\varepsilon$ corresponding to our experiments, the expected movement is 16 μm. The experimentally observed movement was 12 μm.

Implications for the Development of Inflatable Membrane Mirrors

Clearly there is a need for electroactive polymers with far higher electromechanical coupling (actuation capability), and such materials are already under development.[16] The effective strain from such actuators can again be calculated using Eq. (3). The centerpoint

deflection due to actuation can be estimated with sufficient accuracy to conduct a systems-level trade study using Eq. (5). An FEM study could be done subsequently to predict accurately the overall membrane shape correction similar to that shown in Fig. 6.

Conclusions

This paper has provided insight into the magnitude of shape correction possible for inflatable membrane reflectors through cure shrinkage of a rigidizable layer and actuation of a piezo-strictive, that is, PVDF, layer. Results have shown that a limited amount of shape correction is possible with both techniques. However, the magnitude of shape correction diminishes dramatically with inflation pressure and is not sufficient to overcome the surface errors caused by geometric nonlinearities at high inflation pressures, that is, the W error. The paper also provides a basis for the design of electromechanical actuators that could enable further development of inflatable membrane mirror technology.

In particular, a shadow moiré interferometry system was used to study the shape changes of a thin inflated membrane due to shrinkage of a thin epoxy coating during cure. The movement was less than the metrology system resolution of 0.14 mm, which was corroborated with a finite element based study. This result is because the stiffness of the curing epoxy is very low until after most of the cure shrinkage has taken place. This result implies two things. First, the use of cure shrinkage for altering the inflated shape of a rigidizable membrane should be limited to reflector systems with very low inflation pressures. Second, for reflectors with high inflation pressures, the coating stresses from rigidization in space will not significantly affect the membrane shape, for example, beyond what is correctable with active control with PVDF.

It was determined that the experimental apparatus, which involved inflation of the membrane test specimen using a vacuum chamber, allowed systematic micrometer-level movements (per minute) of the membrane due to the permeability of polymeric membrane. This effect made it impossible to study the deformations induced by coating stresses at the micrometer and submicrometer level over timescales relevant for such rigidization experiments. One alternative to be considered in the future is to use a vacuum chamber of significantly greater volume so that the diffusion has a smaller impact on the internal pressure.

Electrical actuation of a membrane with a PVDF film under low inflation pressure showed that the surface movement could be approximately 10 μm as seen using the laser interferometry system. However, unlike a free-standing BiMorph membrane, an inflated membrane will not demonstrate millimeter levels of shape correction, even though it is under minimal inflation pressure. Therefore, this approach is inadequate in correcting for the W error, but could be used for small amount of shape correction.

Acknowledgments

This research was sponsored by the Air Force Office of Scientific Research, Daniel J. Segalman, Program Manager. Patrick Montemerlo was partially supported by the New Mexico State University NASA Space Grant Program.

References

[1]Chmielewski, A. B., "Overview of Gossamer Structure," *Gossamer Spacecraft*, edited by C. H. M. Jenkins, Vol. 191, AIAA, Reston, VA, 2001, pp. 1–33.

[2]Jenkins, C. H., Feeland, R. E., Bishop, J. A., and Sadeh, W. Z., "An Up-to-Date Review of Inflatable Structures Technology for Space-Based Applications," Space 98: 6th International Conf. and Expo on Engineering, Construction, and Operations in Space, American Society of Civil Engineers, Reston, VA, 1998.

[3]Jenkins, C. H., Wilkes, J. M., and Marker, D. K., "Surface Accuracy of Precision Membrane Reflectors," *Sixth International Conference and Exposition on Engineering Construction and Operations in Space*, American Society of Civil Engineers, Reston, VA, 1998, pp. 118–125.

[4]Denoyer, S. J., and Maji, A. K., "Lightweight Adaptable Space Optics: The Advanced Mirror System Demonstrator," *Proceedings of 51st International Astronautical Congress*, Society of Photo-Optical Instrumentation Engineers, Bellingham, WA, 2000.

[5]Guidanean, K., and Williams, G. T., "An Inflatable Rigidizable Truss Structure with Complex Joints," AIAA Paper 98-2105, 1998.

[6]Martin, J. W., Main, J. A., and Nelson, G. C., "Development of a Testbed for Evaluating Electron Gun Shape Correction of Distributed Structures," Adaptive Structures and Materials Symposium, American Society of Mechanical Engineers International Mechanical Engineering Congress and Exposition, 1999.

[7]Maji, A. K., and Starnes, M., "Shape Measurement and Control of Deployable Membrane Structures," *Experimental Mechanics Journal*, Vol. 40, No. 2, 2000, pp. 154–159.

[8]Hung, Y. Y., "Shearography, A Novel and Practical Approach," *Journal of Nondestructive Evaluation*, Vol. 8, No. 2, 1989, pp. 55–67.

[9]Maji, A. K., and Montemerlo, P., "Shape Control of a Deployable Membrane Reflector," Proceedings of the 16th Annual Technical Conf. of the American Society of Composites, Sept. 2001.

[10]Post, D., "Moiré Interferometry," *Handbook on Experimental Mechanics*, edited by A. S. Kobayashi, Society for Experimental Mechanics, Bethel, CT, 1987, pp. 314–350.

[11]Hencky, H., "Uber den Spannungzustand in Kreisrunden Platten," *Zeit. F. Math. U Phys.*, Vol. 63, 1915, pp. 311–317.

[12]Koerner, R. M., *Designing with Geosynthetics*, 3rd ed., Prentice–Hall, Upper Saddle River, NJ, 1995, pp. 430–435.

[13]Daniel, I. M., Wang, T. M., Karalekas, D., and Gotro, J., "Determination of Chemical Cure Shrinkage in Composite Laminates," *Journal of Composite Technology and Research*, Vol. 12, No. 3, 1990, pp. 172–176.

[14]Geuss, T. R., Chambers, R. S., Hinnerichs, T. E., McCarty, G. D., and Shagum, R. N., "Epoxy and Acrylic Stereolithography Resins; Insitu Measurements of Cure Shrinkage and Stress Relaxion," Sandia National Labs., Rept. SAND-94-2569, Albuquerque, NM, 1994.

[15]Timoshenko, S., and Krieger, S. W., *Theory of Plates and Shells*, 2nd ed., McGraw–Hill, New York, 1987, pp. 445–447.

[16]Cheng, Z., Bharti, V., Xu, T., Xu, H., Mai, T., and Zhang, Q., "Electrostrictive Poly (Vinylidene Fluoride Trifluoroethylene) Copolymers," *Sensors and Actuators*, Vol. A90, 2001, pp. 138–147.

M. S. Lake
Associate Editor